Convergence properties of the cluster expansion for equal-time Green functions in scalar theories *

A. Peter, W. Cassing, J.M. Häuser, and M.H. Thoma
Institut für Theoretische Physik, Universität Gießen
35392 Gießen, Germany

February 1, 2008

February 1, 2008

Abstract

We investigate the convergence properties of the cluster expansion of equal-time Green functions in scalar theories with quartic self-coupling in $(0+1)$, $(1+1)$, and $(2+1)$ space-time dimensions. The computations are carried out within the equal-time correlation dynamics approach, which consists in a closed set of coupled equations of motion for connected Green functions as obtained by a truncation of the BBGKY hierarchy. We find that the cluster expansion shows good convergence as long as the system is in a localized state (single phase configuration) and that it breaks down in a non-localized state (two phase configuration), as one would naively expect. Furthermore, in the case of dynamical calculations with a time dependent Hamiltonian for the evaluation of the effective potential we find two timescales determining the adiabaticity of the propagation; these are the time required for adiabaticity in the single phase region and the time required for tunneling into the non-localized lowest energy state in the two phase region. Our calculations show a good convergence for the effective potentials in $(1+1)$ and $(2+1)$ space-time dimensions since tunneling is suppressed in higher space-time dimensions.

PACS: 11.30.Qc; 11.90.+t.

*supported by DFG, Forschungszentrum Jülich and GSI Darmstadt

1 Introduction

The many-body problem of quantum field theory, in spite of great efforts in the past, still remains unsolved and there is a need for genuine nonperturbative methods. In [1] we have proposed a connected (equal-time) Green function approach for SU(N) gauge theories which might provide valuable insight into the low energy QCD problem. However, the possible truncation schemes in the order of the connected Green functions will be limited for practical purposes and one thus needs intrinsic criteria that allow for a judgement of the convergence properties of the approach especially in those cases, where exact solutions are not available.

Before adressing the SU(N) Yang-Mills problem, we analyze the convergence properties of the correlation dynamical approach for the scalar quantum field theory with $\lambda\Phi^4$ self-interaction, which has become an important theoretical laboratory for testing non-perturbative methods. This is partly due to the fact that Φ^4-theory provides an easy framework for studying different scenarios in nonperturbative renormalization when going from $(0+1)$ to $(1+1)$ [2]-[9], $(2+1)$ [7]-[11] and $(3+1)$ [12]-[14] space-time dimensions.

In two preceding articles [15, 16] we have investigated ground state symmetry breaking and the effective potential in Φ^4-theory in $(1+1)$ and $(2+1)$ space-time dimensions using the equal-time correlation dynamics method (in $(d+1)$-dimensional Φ^4-theory denoted as $\Phi^4_{d+1}CD$), which consists in a coupled set of equations of motion for connected equal-time Green functions. This coupled set of equations is obtained by inserting the cluster expansion, i.e. the expansion of full Green functions in terms of connected Green functions, into the equations of the BBGKY hierarchy and by neglecting all connected n-Point functions with $n > N$ for some given N.

The derivation of the correlation dynamical equations for Φ^4-theory has been presented in detail in [15, 16]; the resulting equations in $(1+1)$ dimensions are given by Eqs. (20)-(31) in appendix A of [15] and in $(2+1)$ dimensions by Eqs. (19)-(21) in Sect. 2 as well as Eqs. (28)-(36) in the appendix of [16]. The equations in $(0+1)$ dimensions can easily be obtained from those in higher dimensions by discarding the dependence on the spatial coordinates and by omitting all mass counterterms. For a more general discussion of correlation dynamics in case of nonrelativistic fermionic systems we refer the reader to refs. [17, 18, 19, 20].

The calculations in [15, 16] aimed at the evaluation of the effective potential $V_{eff}(\Phi_0)$, which is given by the minimum of the energy expectation value in the subspace of states with a fixed expectation value of the scalar field $\langle\Phi\rangle = \Phi_0$. Since the $\Phi^4_{d+1}CD$-equations describe the (equal-time) evolution of the system for a given initial condition, a direct (variational) evaluation of the effectiv potential within this approach would amount to minimizing the energy in the manifold of stationary solutions with the constraint $\langle\Phi\rangle = \Phi_0$. In practice, however, this turns out to be impossible because the energy is not bounded from below without additional constraints, since the solution manifold

contains unphysical Green functions. Although e.g. for the $(0+1)$-dimensional case in the 2-point approximation a sufficient constraint can be derived from the uncertainty relation, it is not yet clear what constraints for higher order approximations have to be imposed.

The computation of the effective potential and the corresponding lowest energy state Green functions within our approach is therefore carried out by means of a dynamical calculation using the Gell-Mann and Low theorem, i.e. by adiabatically changing the parameters of the theory in time from a configuration with a well known lowest energy state solution to the actual configuration of interest as described in [15, 16]. Whereas this many-body scheme was found to converge quite rapidly in case of nonrelativistic nuclear physics problems [20], it is not clear if this also holds for the quantum field theoretical case. We thus have to explore the convergence of the cluster expansion and its dependence on the parameters of the theory, i.e. the coupling λ and the expectation value of the scalar field $\langle\Phi\rangle = \Phi_0$.

Before investigating Φ^4-theory in $(1+1)$ and $(2+1)$ space-time dimensions, we turn to the simpler case of $(0+1)$ space-time dimensions, which is equivalent to the quantum mechanical anharmonic oscillator in case of a positive squared mass and to the quantum mechanical double-well potential in case of a negative squared mass. Since in $(0+1)$ dimensions we have access to the exact lowest energy state solution for given $\langle \mathrm{x}\rangle = \mathrm{x}_0$, we here can also directly control the validity of the correlation dynamical solution.

This article is organized as follows: In Sect. 2 we investigate the $(0+1)$-dimensional case in full detail with respect to the problem of degenerate vacua and quantum tunneling, whereas in Sect. 3 we present our numerical results for the $(1+1)$- and the $(2+1)$-dimensional case. Sect. 4 concludes the present study with a brief summary of our results, while technical details of the cluster expansion as well as the GEP (Gaussian effective potential) approximation are given in appendices A to C.

2 Convergence of the cluster expansion in $(0+1)$ dimensions

In $(0+1)$ space-time dimensions and with the identification $\Phi(t) \to \mathrm{x}(t)$, $\Pi(t) \to \mathrm{p}(t)$, the Lagrangian of Φ^4-theory with positive squared mass m^2 (anharmonic oscillator) reads

$$L_1 = \frac{1}{2}(\partial_t \mathrm{x})^2 - \frac{1}{2}m^2\mathrm{x}^2 - \frac{1}{4}\lambda\mathrm{x}^4 \,, \tag{1}$$

while the Hamiltonian is given by

$$H_1 = \frac{1}{2}\mathrm{p}^2 + \frac{1}{2}m^2\mathrm{x}^2 + \frac{1}{4}\lambda\mathrm{x}^4 \tag{2}$$

with the usual equal-time commutation relation $[\mathrm{x}(t), \mathrm{p}(t)] = i$.

In case of a negative squared mass $m^2 = -\mu^2$ (double-well potential) we write the Lagrangian and the Hamiltonian as

$$L_2 = \frac{1}{2}(\partial_t \mathrm{x})^2 + \frac{1}{2}\mu^2 \mathrm{x}^2 - \frac{1}{4}\lambda \mathrm{x}^4 - \frac{\mu^4}{4\lambda} = \frac{1}{2}(\partial_t \mathrm{x})^2 - \frac{1}{4}\lambda(\mathrm{x}^2 - \frac{\mu^2}{\lambda})^2 \tag{3}$$

and

$$H_2 = \frac{1}{2}\mathrm{p}^2 + \frac{1}{4}\lambda(\mathrm{x}^2 - \frac{\mu^2}{\lambda})^2 \ . \tag{4}$$

Since we are aiming at the effective potential, i.e. the properties of the system not only as a function of the coupling λ, but also as a function of $\langle \mathrm{x} \rangle = \mathrm{x}_0$, we explicitly split off the vacuum expectation value by writing

$$\mathrm{x} = x + \mathrm{x}_0 \ , \quad \langle x \rangle = 0 \ ; \quad \mathrm{p} = p \tag{5}$$

and treat x_0 as a constant classical background field which can be varied as an external parameter. The explicit $\Phi^4_{0+1}CD$ equations then are obtained in the usual way, i.e. by inserting the cluster expansion (cf. appendix A) into the coupled set of equations of motion for the n-point Green functions $\langle xx \rangle$, $\langle px \rangle$, $\langle pp \rangle$, $\langle xxx \rangle$, $\langle pxx \rangle$, $\langle ppx \rangle$, $\langle ppp \rangle$, etc. The resulting set of coupled equations for the connected Green functions $\langle xx \rangle_c$, $\langle px \rangle_c$, $\langle pp \rangle_c$, ..., then can be closed by neglecting connected Green functions above some order $n > N$, where N is an integer ≥ 2. Since the resulting set of equations is quite lengthy and in case of $N = 4$ has been presented in refs. [15, 16] for $(1+1)$ and $(2+1)$ dimensions, we omit an explicit representation here.

In order to investigate the convergence of the cluster expansion, we compute the quantities

$$|\langle \mathrm{x}^n \rangle_c / \langle \mathrm{x}^n \rangle| \ , \tag{6}$$

where $\langle \cdot \rangle_c$ stands for the connected part of the expectation value $\langle \cdot \rangle$ (cf. appendix B) for $n = 2,\ 3,\ 4,\ 5,\ 6$ in the exact lowest energy state solution as well as in the $\Phi^4_{0+1}CD$ approach using a 6-point truncation scheme, i.e. including the connected n-point functions with $n \leq 6$. In line with the notations in [15, 16] this set of equations is denoted by $\Phi^4_{0+1}CD(2,3,4,5,6)$.

In our analysis we consider two quite distinct cases; i.e. an extreme double-well potential with $\lambda/(4\mu^3) = 0.0158$ and an anharmonic oscillator potential with $\lambda/(4m^3) = 10$. The values (6) of the exact solution have been obtained by diagonalizing the Hamiltonian of the system with an additional external source (cf. (8)) in a sufficiently large set of basis states. The $\Phi^4_{0+1}CD(2,3,4,5,6)$-results have been obtained in the usual way by exploiting the Gell-Mann and Low theorem. We start

with the GEP solution [7, 15, 21] (cf. appendix C) and switch on the residual interaction terms adiabatically. In case of the anharmonic oscillator this corresponds to a time-dependent Hamiltonian of the form

$$H(t) = \frac{1}{2}\mathrm{p}^2 + \frac{1}{2}M^2\mathrm{x}^2 + \frac{g(t)}{\lambda}\left[\frac{m^2 - M^2}{2}\mathrm{x}^2 + \frac{1}{4}\lambda\mathrm{x}^4\right] , \tag{7}$$

where the residual coupling $g(t)$ runs from zero to λ, M is the effective mass of the GEP-solution and x_0 is fixed. We recall that in the correlation dynamical calculation the 1-point functions $\langle x\rangle$ and $\langle p\rangle$ are set equal to zero according to (5), and for each value of x_0 an individual time dependent calculation has to be carried out. We have used a linear time dependence of the form $g(t)/4\mu^3 = \beta t$ or $g(t)/4m^3 = \beta t$, respectively, where β in each case has been chosen sufficiently small such that the system shows adiabatic convergence as long as x_0 is outside the domain where the exact solution indicates a breakdown of the cluster expansion. Our numerical results for (6) in the lowest energy state with given expectation value x_0 are shown in Fig. 1 as a function of x_0 for both potentials. The explicit results from the exact solution are displayed on the l.h.s. whereas the r.h.s. shows the corresponding quantities in $\Phi^4_{0+1}CD(2,3,4,5,6)$ approximation. We note that the sharp peaks for certain values of $\mathrm{x}_0/\sqrt{m}$ or $\mathrm{x}_0/\sqrt{\mu}$ in Fig. 1 result from a change of sign of $\langle \mathrm{x}^n\rangle_c/\langle \mathrm{x}^n\rangle$.

In the case of the double-well potential the exact solution (upper left part of Fig. 1) yields a dramatic sudden change in the relative importance of the connected Green functions at a value of $\mathrm{x}_0^{crit}/\sqrt{\mu} \approx 3.8$. Above $\mathrm{x}_0^{crit}/\sqrt{\mu}$ the relative importance of the connected Green functions decreases by at least one order of magnitude as one goes from n to $n+1$, implying an excellent convergence of the cluster expansion. In contrast to that, in the region below $\mathrm{x}_0^{crit}/\sqrt{\mu}$ the full Green functions are dominated by their connected parts, i.e. the system is dominated by fluctuations.

The corresponding result in $\Phi^4_{0+1}CD(2,3,4,5,6)$-approximation (upper right part of Fig. 1) above $\mathrm{x}_0^{crit}/\sqrt{\mu}$ shows nearly the same result as the exact solution. This has been expected due to the excellent convergence of the cluster expansion in this region. The sudden rise in the relative importance of the higher order connected Green functions in going from $\mathrm{x}_0/\sqrt{\mu} > \mathrm{x}_0^{crit}/\sqrt{\mu}$ to $\mathrm{x}_0/\sqrt{\mu} < \mathrm{x}_0^{crit}/\sqrt{\mu}$, however, is smeared out over an extended region for the finite value of β taken in the calculation. However, it becomes evident that as soon as the connected Green functions dominate the full Green functions ($\mathrm{x}_0/\sqrt{\mu} \approx 2.84$), the method of time dependently switching on the residual interaction within the $\Phi^4_{0+1}CD(2,3,4,5,6)$-approximation breaks down.

In contrast to the results for the double-well potential, the ratios (6) for the anharmonic oscillator (lower two pictures in Fig. 1) demonstrate a good agreement between the exact solution and the $\Phi^4_{0+1}CD(2,3,4,5,6)$-solution for all $\mathrm{x}_0/\sqrt{\mu}$. The relative importance of the connected Green functions increases with decreasing $\mathrm{x}_0/\sqrt{\mu}$, but even at $\mathrm{x}_0/\sqrt{\mu} = 0$ the higher order full Green functions can in a good approximation be expressed by their disconnected parts (note that $\langle \mathrm{x}^2\rangle_c/\langle \mathrm{x}^2\rangle \to 1$ as $\mathrm{x}_0 \to 0$ by

definition).

In order to understand the numerical results for the double well potential in Fig. 1 in a more qualitative way, we now examine the wave functions obtained by the exact solution for the system. We first note that instead of finding the lowest energy state in the subspace of all states with given $\langle \mathrm{x} \rangle = \mathrm{x}_0$, one can equivalently introduce a source term into the Hamiltonian by writing

$$H_2^J = H_2 - \mu J \mathrm{x} \tag{8}$$

and then find the ground state of the system with respect to the whole Hilbert space. The resulting state, which has some vacuum expectation value $\mathrm{x}_0(J)$ depending on the source J, is also the lowest energy state in the subspace with given $\mathrm{x}_0(J)$.

In Fig. 2 we display the absolute square of the ground state wavefunction $\Psi_0(\mathrm{x})$ and the wavefunction of the first excited state $\Psi_1(\mathrm{x})$ of the Hamiltonian (8) with $\lambda/(4\mu^3) = 0.0158$ as a function of $f(J) = \mathrm{x}_0(J)/\sqrt{\mu}$ and $\mathrm{x}/\sqrt{\mu}$ where both wavefunctions have been obtained via diagonalization of (8). At $f(J) = 0$, $|\Psi_0(\mathrm{x})^2|$ and $|\Psi_1(\mathrm{x})^2|$ have approximately the same shape with maxima at $\pm \mathrm{x}^{min}$. We note that in the limit $\lambda/(4\mu^3) \to 0$ the double-well potential develops an infinitely high barrier at $\mathrm{x} = 0$. This leads to a spectrum of the Hamiltonian for $J = 0$ which consists of pairs of degenerate Eigenvalues. Due to the infinite barrier at $\mathrm{x} = 0$ there is no more tunneling between the 2 orthogonal states spanning the Eigenspace corresponding to each Eigenvalue. The lowest energy states of the system then are of the form

$$|\Psi_0\rangle = a|L_0\rangle + b|R_0\rangle \tag{9}$$

with $|L_0\rangle$ and $|R_0\rangle$ denoting the mutually orthogonal lowest energy solutions with $\langle L_0|\mathrm{x}|L_0\rangle = -\mathrm{x}^{min}$ and $\langle R_0|\mathrm{x}|R_0\rangle = +\mathrm{x}^{min}$, i.e. the optimally localized "left" and "right" states which can be constructed from an appropriate superposition of the degenerate ground states. We then obtain

$$\langle \Psi_0|\mathrm{x}|\Psi_0\rangle = \mathrm{x}^{min}(|b|^2 - |a|^2) \ \in [-\mathrm{x}^{min}, \mathrm{x}^{min}] \tag{10}$$

with $\langle L_0|\mathrm{x}|R_0\rangle = 0$; states of the form (9) thus restore the convex shape of the effective potential by making it flat between $-\mathrm{x}^{min}$ and x^{min}. As soon as $J \neq 0$, the system will energetically prefer to shift its ground state wavefunction completely to one side of the potential barrier, depending on the sign of J. In other words, the system with an infinitely high potential barrier undergoes a phase transition from the state $|L_0\rangle$ to the state $|R_0\rangle$ as J passes through zero. Here we use the term "phase transition" for any discontinuous behaviour of the lowest energy solution with respect to the parameters of the Hamiltonian.

If $\lambda/(4\mu^3)$ assumes a finite (but still small) value as in case of Fig. 2, the pairwise degeneracy of Eigenvalues disappears due to tunneling – which is no longer forbidden for finite λ – but the spectrum still consists of pairs with a small energy gap. The

separation of the lowest Eigenvalues $\Delta E = E_1 - E_0$ can be taken as a measure of the inverse tunneling time. The region between $-\mathrm{x}^{min}$ and x^{min} then can be covered by a very small variation of J, i.e. the above obtained "phase transition" from $|L_0\rangle$ to $|R_0\rangle$ at $J = 0$ in case of a finite coupling is smeared out into a sharp crossover. As can be seen from Fig. 2, the ground state wavefunctions are (to a very good approximation) still of the form (9), with only slight modifications due to tunneling. The first excited state of the system then is given by the Eigenstate corresponding to the higher Eigenvalue in the lowest lying pair, i.e. approximately by

$$|\Psi_1\rangle = b^*|L_0\rangle - a^*|R_0\rangle \ . \tag{11}$$

In Fig. 2, this can be seen from the fact that the relative strengths of the left and right maxima of $|\Psi_1(\mathrm{x})^2|$ and $|\Psi_0(\mathrm{x})^2|$ depend on $f(J)$ in exactly the opposite way.

For $|f(J)| > \mathrm{x}^{min}/\sqrt{\mu}$ the system suddenly changes its behaviour and the ground state and the first excited state are localized states, which to a good approximation can be described as the ground state and the first excited state of the harmonic oscillator potential obtained in second order Taylor expansion of the classical potential around its minima, as can also be observed in Fig. 2. This corresponds to the single phase localized configuration at finite J in the limiting case of the infinitely high potential barrier.

We arrive at the conclusion that for a finite, but small value of $\lambda/(4\mu^3)$ – although the system does not exhibit true ground state symmetry breaking due to tunneling –, it will still qualitatively behave like a system which is in a (non-localized) two phase configuration for $|\mathrm{x}_0| < \mathrm{x}^{min}$ and in a (localized) single phase configuration for $|\mathrm{x}_0| > \mathrm{x}^{min}$.

It is now straightforward to show analytically, that the cluster expansion has to break down in a two phase configuration according to (9) as soon as it shows good convergence in both optimally localized single phase configurations. Furthermore, in a field theory with an arbitrary space-time dimensionality, the cluster decomposition property of the connected Green functions,

$$G_n^c(x_1, \cdots, x_p; y_{p+1}, \cdots, y_n) \to 0 \quad \left(\min_{\substack{i=1,\cdots,p \\ j=p+1,\cdots,n}} |x_i - y_j| \to \infty \right) \ , \tag{12}$$

is lost in a state constructed according to (9) whenever $|L_0\rangle$ and $|R_0\rangle$ are the optimally localized states in case of a system with ground state symmetry breaking. For the (0+1) dimensional system this has no direct implication for equal-time Green functions since it only applies to the time arguments, e.g. in a time ordered Green function.

Taking into account the above considerations, we can now identify x^{min}, the expectation value of x in the optimally localized right state, with x_0^{crit}, for which (6) (cf. the upper left part of Fig. 1) shows a relatively sharp rise. In the correlation dynamical calculation (displayed in the upper right part of Fig. 1), the sharp rise is smeared out.

We also observe that the region, in which the system is dominated by fluctuations, only extends up to $x_0/\sqrt{\mu} \approx 3.3$ instead of $x_0/\sqrt{\mu} = x_0^{crit} \approx 3.8$ for the exact solution.

In order to get an explanation for this behaviour, we show in Fig. 3 a qualitative picture of the external source J as a function of x_0 for 3 different cases. In case (1) (dashed line), there is no ground state symmetry breaking and for each value of J there is a unique value $x_0(J)$. In case (2), furthermore, we have the situation corresponding to the convex shape of the effective potential given by the construction of nonlocal states (9) in case of ground state symmetry breaking, where for any nonzero value of J there is a unique value $x_0(J)$ and for $J = 0$ all values between $-x^{min}$ and x^{min} are accessible. This corresponds to the field theoretical Maxwell construction [22], where the two phases, given by the left and the right optimally localized state in (9) "coexist". In case (3) we still have ground state symmetry breaking, but the curve for $J(x_0)$ is analytically continued into the region, where the field theoretical Maxwell construction takes place, implying that no phase coexistence is allowed here.

Due to the non-ergodicity of a system, that posesses 2 phases without tunneling in between, the trajectory of case (3) is realized in any time dependent adiabatic process as used in our correlation dynamics approach for the computation of the effective potential. This results in a good convergence of the cluster expansion throughout the whole process, because the system always stays in a localized state. For the double-well potential with finite potential barrier this is e.g. realized within the $\Phi^4_{0+1}CD(2)$-limit, i.e. the time-dependent Hartree-Fock method, because at this level of approximation tunneling is not yet included. The adiabatic limit of the $\Phi^4_{0+1}CD(2)$ solution then simply is the GEP solution, i.e. the lowest energy Gaussian.

However, for a system with tunneling between the 2 phases we come to the conclusion that the convergence properties of the cluster expansion with respect to the adiabatic computation of the lowest energy state are determined by the relative magnitude of 2 timescales: the specific tunneling time t_{tun} and the time t_{prop} over which the system is propagated; the latter quantity in our case is always chosen to ensure sufficient adiabatic convergence in the single phase region. The tunneling time for a given system itself depends on the correlation dynamical truncation scheme; as indicated above, t_{tun} is always infinite within the 2-point truncation scheme and the inclusion of higher order connected Green functions will in general tend to decrease it.

If $t_{tun} \gg t_{prop}$, a dynamical phase mixing will be negligible and our correlation dynamics will give useful results for the dynamical time evolution of the system. In the two phase region, however, the system will no longer propagate along an adiabatic trajectory of lowest energy. Loosely speaking, the correlation dynamical time evolution will generate states of lowest energy in the "subspace of sufficiently localized states", the latter of course not being mathematically well defined.

On the other hand, for $t_{tun} \lesssim t_{prop}$ tunneling will lead to a breakdown of correlation dynamics in the course of the time integration. This is the reason for the breakdown of the $\Phi^4_{0+1}CD(2,3,4,5,6)$ approach for $x_0/\sqrt{\mu} \lesssim 3.3$ in the upper right part of Fig. 1.

In order to investigate the behaviour of our double-well system with respect to the different time scales in a manner directly related to the idealized picture given in Fig. 3, we now choose a different dynamical process, in which the background field x_0 is changed as a function of time. For the initialization at $t = 0$ we make use of the fact that for $\mathrm{x}_0 \to \infty$ (strong field limit) the system approaches the classical limit; there again the GEP solution can be taken as a starting configuration even though the residual interaction is completely taken into account in the time propagation right from the beginning.

We then compute the corresponding external source J as a function of x_0 by imposing the Hellmann-Feynman theorem (which of course strictly only holds for an exact Eigenstate of the system)

$$\begin{aligned}\frac{d}{dJ}E_0(J) = \frac{d}{dJ}\langle\Psi_0(J)|H_2^J|\Psi_0(J)\rangle &= \langle\Psi_0(J)|\frac{d}{dJ}H_2^J|\Psi_0(J)\rangle \\ &= -\mu\langle\Psi_0(J)|\mathrm{x}|\Psi_0(J)\rangle = -\mu\mathrm{x}_0(J)\ , \end{aligned} \tag{13}$$

where H_2^J is given by (8). Inserting (8) into (13) yields

$$-\mu\mathrm{x}_0(J) = \frac{d}{dJ}\langle H_2^J\rangle = \frac{d}{dJ}\langle H_2\rangle - \mu\mathrm{x}_0(J) - \mu J\frac{d}{dJ}\mathrm{x}_0(J)\ . \tag{14}$$

With

$$\frac{d}{dJ}\langle H_2\rangle = \left(\frac{d}{d\mathrm{x}_0}\langle H_2\rangle\right)\left(\frac{d}{dJ}\mathrm{x}_0(J)\right) \tag{15}$$

we obtain

$$J(\mathrm{x}_0) = \frac{1}{\mu}\frac{d}{d\mathrm{x}_0}\langle H_2\rangle \tag{16}$$

relating the external source J to the effective potential in the usual way. The philosophy behind this definition of $J(\mathrm{x}_0)$ within a dynamical calculation is the interpretation already indicated above, that for $t_{tun} \gg t_{prop}$ the system will "quasi-adiabatically" evolve in the subspace of localized (single phase) states.

In Fig. 4 the external source J is plotted as a function of $\mathrm{x}_0/\sqrt{\mu}$ in $\Phi^4_{0+1}CD(2,3,4,5,6)$-approximation for a double-well potential with $\lambda/(4\mu^3) = 0.0158$, where x_0 has been changed in time according to $\mathrm{x}_0(t)/\sqrt{\mu} = \mathrm{x}_0^{start}/\sqrt{\mu} - \alpha t$. The fat solid line is the result in $\Phi^4_{0+1}CD(2)$-approximation with $\alpha = 0.00001$ c/fm ($\mu^2 = 1$ MeV^2), which essentially lies on top of the GEP result and is shown for comparison. For large values of α the trajectory in the $(J - \mathrm{x}_0)$–plane can be computed down to $\mathrm{x}_0 = 0$ without any problem and exhibits the same qualitative behaviour as the trajectory of case (3) in Fig. 3, indicating that for $\alpha > 0.01024$ c/fm we have $t_{tun} \gg t_{prop} \propto 1/\alpha$.

By reducing α we get into the region where $t_{tun} \approx t_{prop}$. The inclusion of higher order connected Green functions then allows for tunneling, thus leading to a breakdown

of the dynamical time propagation due to the dominance of fluctuations in the phase coexistence regime. With decreasing α, the value of x_0, at which this breakdown happens, shifts towards the point where J changes sign ($x_0 \approx 3.8$). In the exact solution this value corresponds to the boundary of the phase coexistence region (cf. upper left part of Fig. 1).

3 Convergence of the cluster expansion in $(1+1)$ and $(2+1)$ dimensions

We now turn to the technically much more involved case of $(1+1)$- and $(2+1)$-dimensional Φ^4-theory. Both theories are superrenormalizable, and only a mass renormalization is required. The Lagrangian and the Hamiltonian are given by

$$\mathcal{L} = \frac{1}{2}\partial_\mu\Phi\partial^\mu\Phi - \frac{1}{2}m_0^2\Phi^2 - \frac{1}{4}\lambda\Phi^4 \,, \tag{17}$$

$$H = \frac{1}{2}\int d^\nu x \left[\Pi^2 + (\nabla\Phi)^2 + m_0^2\Phi^2 + \frac{1}{2}\lambda\Phi^4\right] \,, \tag{18}$$

where $m_0^2 = m^2 + \delta m^2$ is the bare mass, m^2 the renormalized mass and ν denotes the number of spatial dimensions. δm^2 contains the mass counterterms, which in $(2+1)$ dimensions are given by the tadpole diagram and the setting sun diagram, and in $(1+1)$ dimensions by the tadpole diagram only (cf. [15, 16]).

The field operators and their conjugate momenta are expanded into plane waves in a box with periodic boundary conditions according to

$$\Phi(x) = \sum_\alpha \Phi_\alpha\psi_\alpha(x) \,, \quad \Pi(x) = \sum_\alpha \Pi_\alpha\psi_\alpha(x) \tag{19}$$

with $\psi_\alpha(x) = \frac{1}{\sqrt{V}}e^{i\vec{k}_\alpha\vec{x}}$; $V = L^\nu$ and $\vec{k}_\alpha$ chosen according to the boundary conditions.

For our numerical simulations in $(1+1)$ dimensions we use $L = 100$ fm, $m = 10$ MeV and the 21 lowest lying plane waves; in $(2+1)$ dimensions we use $L = 20$ fm, $m = 10$ MeV and the 29 lowest lying states. For further details of the explicit set of equations solved we refer the reader to refs. [15, 16].

In Fig. 5 we show the quantities

$$\left|\sum_{\alpha\beta}\langle\Phi_\alpha\Phi_\beta\rangle_c \,/\, \sum_{\alpha\beta}\langle\Phi_\alpha\Phi_\beta\rangle\right| = \left|\langle\Phi^2(x)\rangle_c \,/\, \langle\Phi^2(x)\rangle\right| \;\; (n=2) \,, \tag{20}$$

$$\left|\sum_{\alpha\beta\gamma}\langle\Phi_\alpha\Phi_\beta\Phi_\gamma\rangle_c \,/\, \sum_{\alpha\beta\gamma}\langle\Phi_\alpha\Phi_\beta\Phi_\gamma\rangle\right| = \left|\langle\Phi^3(x)\rangle_c \,/\, \langle\Phi^3(x)\rangle\right| \;\; (n=3) \tag{21}$$

and

$$\left| \sum_{\alpha\beta\gamma\delta} \langle \Phi_\alpha \Phi_\beta \Phi_\gamma \Phi_\delta \rangle_c \; / \sum_{\alpha\beta\gamma\delta} \langle \Phi_\alpha \Phi_\beta \Phi_\gamma \Phi_\delta \rangle \right| = \left| \langle \Phi^4(x) \rangle_c \; / \; \langle \Phi^4(x) \rangle \right| \;\; (n=4) \; , \tag{22}$$

as a function of $\Phi_0 = \langle \Phi(x) \rangle = L^{-\nu/2} \langle \Phi(\vec{k} = \vec{0}) \rangle$. Note that due to translation invariance all Green functions with $\sum_{\alpha_i} \vec{k}_{\alpha_i} \neq \vec{0}$ have to vanish. The quantities (20), (21) and (22) have been chosen as a measure for the relative importance of the higher order connected Green functions in analogy to (6). All results have been obtained within the $\Phi^4_{\nu+1} CD(2,3,4)$-approximation (i.e. including everything up to the connected 4-point function), which is the lowest order in correlation dynamics to which the setting sun diagram contributes, which diverges logarithmically in (2+1) dimensions (cf. [16]). The coupling has been switched on in time according to

$$\frac{\lambda}{4m^{3-\nu}} = \beta t \tag{23}$$

with the free (perturbative vacuum) solution as initialization. This method is more efficient than switching on the residual interaction with the GEP solution as an initialization, since it yields results for the lowest energy state over a whole range of coupling constants in only a single time dependent run. In the $(0+1)$-dimensional case, the method of switching on the residual interaction (leading to a correlated state for only one value of the coupling constant) had to be chosen, because the double well potential has no "unperturbed phonon state", because for zero coupling the potential is a harmonic oscillator with negative mass and thus not bounded from below. The vacuum expectation value Φ_0 has been split off as a classical background field and the 1-point function has not been propagated explicitly in analogy to the treatment of x_0 in the $(0+1)$-dimensional case. The value $\beta = 0.05$ c/fm has been chosen small enough in order to observe an adiabatic behaviour of the time dependent solution.

The results for $(1+1)$ dimensions are shown in the left column and those for $(2+1)$ dimensions in the right column of Fig. 5 for various values of the coupling constant. As in Fig. 1, the peaks result from taking the absolute value of a quantity that changes sign and have no physical meaning. In both, $(1+1)$ and $(2+1)$ dimensions, the relative importance of the connected 3- and 4-point functions increases with increasing coupling and decreasing Φ_0; however, for all parameters considered this relative importance decreases in going from n to $n+1$, and moreover, the highest contribution of the connected 3-point function to the full 3-point function is only about 20 %. The cluster expansion thus shows satisfactory convergence throughout the investigated parameter range.

The critical couplings for a transition into the symmetry broken phase in $(1+1)$ and $(2+1)$ dimensions within the $\Phi^4_{\nu+1} CD(2,3,4)$-approximation are (for the present specific choice of numerical parameters specifying the plane wave basis set) $\lambda/4m^2 = 2.247$ and $\lambda/4m = 0.369$, respectively [15, 16]. Below these couplings a good convergence of

the cluster expansion can be expected, since the system is in a single phase, i.e. it can be described by a localized wave functional. The fact, that we still observe this convergence above the critical coupling indicates that the time t_{tun} required for building up a two phase configuration via tunneling within the $\Phi^4_{\nu+1}CD(2,3,4)$-approximation is infinite or at least large compared to the time t_{prop} needed for the "quasiadiabatic" propagation of the system along the lowest energy localized state trajectory in the sense of Sect. 2. In the latter case, the system would (over a certain range of $t_{prop} \propto 1/\beta$) seem to converge against an asymptotic configuration as t_{prop} increases, and then suddenly change its behaviour when tunneling kicks in. We have only been able to observe such a behaviour in the $(0+1)$ dimensional case, but within the investigated range of β-values not in $(1+1)$ and $(2+1)$ dimensions.

In fact, it is well known that tunneling is suppressed as the number of space-time dimensions increases. In $(1+1)$ dimensions, by means of a soliton-antisoliton pair, it can be shown that tunneling between the two vacua with $\Phi_0 = \pm\Phi_0^{min}$ is still possible [7]. In $(2+1)$ dimensions, however, no tunneling is expected [7]; this would be the lowest space-time dimension with real ground state symmetry breaking, i.e. with an effective potential which is flat between $-\Phi_0^{min}$ and $+\Phi_0^{min}$.

A simple qualitative argument [7] pointing towards the suppression of tunneling in higher space-time dimensions is the following: Consider a bubble of phase 1 within a region of phase 2. The surface region of this bubble then has a higher energy density than the surrounding. In $(1+1)$ dimensions, the surface region is given by the environment of the two end-points of the bubble interval (the soliton and the antisoliton) and its size is therefore independent of the size of the bubble; consequently the bubble can expand without increasing the total energy of the system. Generally, in $(d+1)$ dimensions, the size of the surface region behaves as R^{d-1}, so that for $d \geq 2$ the bubble cannot expand without a corresponding increase in the total energy density. The above geometrical considerations are similar to those used for the proof of Derrick's theorem [23] (non-existence of topological solitons in scalar theories with $d \geq 2$), where a rescaling of the classical field according to $\Phi(x) \to \Phi(\Lambda x)$ is used to show that any potential topological soliton solution would be energetically unstable against variation of Λ.

4 Summary

In this work we have explored the convergence properties of the cluster expansion approach and presented criteria within the theory itself, that allow to conclude about its convergence also in those cases, where the exact solution is not known. As an example we have studied scalar theories with quartic self coupling in $(0+1)$, $(1+1)$, and $(2+1)$ dimensions. We have emphasized the aspect of a nonperturbative computation of the lowest energy state with given field expectation value, since our previous work

[15, 16] aimed at the evaluation of the effective potential.

The Φ^4 theory in $(0+1)$ dimensions is equivalent to a quantum mechanical anharmonic oscillator for positive squared mass and a quantum mechanical double-well potential for negative squared mass. In the case of an anharmonic oscillator with $\lambda/(4m^3) = 10$ we obtained a good convergence of the cluster expansion as well as an excellent agreement between the exact solution and the correlation dynamical solution; this could be explained by the fact that the system is in a single phase (localized state) configuration.

In case of an extreme double-well potential with $\lambda/(4\mu^3) = 0.0158$ the cluster expansion in the exact solution breaks down as soon as the ground state for a given expectation value $\langle \mathrm{x} \rangle$ can approximately be described by a Maxwell construction, i.e. by a coherent superposition of two single phase configurations. The shrinking of the region with dominant fluctuations within the correlation dynamical calculation could be traced back to the fact, that the time t_{prop}, chosen according to the requirement of an adiabatic propagation in the single phase region, is small compared to the tunneling time t_{tun} of the system for certain values of $\langle \mathrm{x} \rangle$.

Our analysis for the QFT systems in $(1+1)$ and $(2+1)$ dimensions demonstrated, that even in the phase coexistence (non-localized state) region, i.e. for coupling constants higher than the critical coupling for ground state symmetry breaking, the correlation dynamical approach yields a good convergence of the cluster expansion. Here, the tunneling times within our dynamical calculation are infinite or at least very large compared to the time required for an adiabatic propagation; this behaviour is traced back to the fact that tunneling is suppressed in $(1+1)$ dimensions and probably absent in $(2+1)$ dimensions.

The main result of this article can therefore be summarized as follows: the applicability of correlation dynamics (which is based on an expansion in terms of connected Green functions) to the adiabatic computation of the lowest energy state with given field expectation value is given if a) the exact stationary solution is a single phase, and b) if the required propagation time for adiabatic or "quasiadiabatic" (cf. Sect. 2) convergence is small compared to the tunneling time. This is in fact the case in higher space-time dimensions since there tunneling is progressively suppressed. This is not only important for lowest energy state calculations as carried out in this article, but also for applications of correlation dynamics to the nonequilibrium dynamics of systems with phase transitions. Furthermore, the relative ratios (20-22) provide an intrinsic test of the correlation dynamical method also for those field theoretical problems, where the exact solution is not known.

A The cluster expansion

The explicit form of the cluster expansion can be derived from the generating functionals of full and connected Green functions (cf. e.g. [15]), $Z[J,\sigma]$ and $W[J,\sigma]$, given by

$$Z[J,\sigma] = \mathrm{Tr}\left\{\rho T\left[e^{i\int d^{\nu+1}x(J(\hat{x})\Phi(\hat{x})+\sigma(\hat{x})\Pi(\hat{x}))}\right]\right\} \tag{24}$$

and

$$Z[J,\sigma] = e^{W[J,\sigma]}\,, \tag{25}$$

respectively, where T is the time ordering operator, ρ is the statistical density operator describing the state of the system ($\mathrm{Tr}\rho = 1$) and $\hat{x}$ denotes (x,t). We start with the cluster expansions for the time-ordered Green functions:

$$\langle\Phi(\hat{x})\rangle \;=\; \langle\Phi(\hat{x})\rangle_c \;, \quad \langle\Pi(\hat{x})\rangle \;=\; \langle\Pi(\hat{x})\rangle_c \;, \tag{26}$$

$$\begin{aligned}
\langle T\Phi(\hat{x}_1)\Phi(\hat{x}_2)\rangle &= \lim_{J,\sigma\to 0}\frac{\delta}{i\delta J(\hat{x}_1)}\frac{\delta}{i\delta J(\hat{x}_2)}e^{W[J,\sigma]} \\
&= \lim_{J,\sigma\to 0}\frac{\delta}{i\delta J(\hat{x}_1)}\left\{\left(\frac{\delta}{i\delta J(\hat{x}_2)}W[J,\sigma]\right)e^{W[J,\sigma]}\right\} \\
&= \lim_{J,\sigma\to 0}\left\{\left(\frac{\delta}{i\delta J(\hat{x}_1)}\frac{\delta}{i\delta J(\hat{x}_2)}W[J,\sigma]\right)+\left(\frac{\delta}{i\delta J(\hat{x}_1)}W[J,\sigma]\right)\left(\frac{\delta}{i\delta J(\hat{x}_2)}W[J,\sigma]\right)\right\}e^{W[J,\sigma]} \\
&= \langle T\Phi(\hat{x}_1)\Phi(\hat{x}_2)\rangle_c + \langle\Phi(\hat{x}_1)\rangle\langle\Phi(\hat{x}_2)\rangle\,,
\end{aligned} \tag{27}$$

where $\langle\cdot\rangle_c$ denotes the connected part of the expectation value. Analogously we obtain

$$\langle T\Pi(\hat{x}_1)\Phi(\hat{x}_2)\rangle = \langle T\Pi(\hat{x}_1)\Phi(\hat{x}_2)\rangle_c + \langle\Pi(\hat{x}_1)\rangle\langle\Phi(\hat{x}_2)\rangle\,,$$

$$\langle T\Pi(\hat{x}_1)\Pi(\hat{x}_2)\rangle = \langle T\Pi(\hat{x}_1)\Pi(\hat{x}_2)\rangle_c + \langle\Pi(\hat{x}_1)\rangle\langle\Pi(\hat{x}_2)\rangle\,,$$

$$\begin{aligned}
\langle T\Phi(\hat{x}_1)\Phi(\hat{x}_2)\Phi(\hat{x}_3)\rangle \;=\; &\langle T\Phi(\hat{x}_1)\Phi(\hat{x}_2)\Phi(\hat{x}_3)\rangle_c + \langle T\Phi(\hat{x}_1)\Phi(\hat{x}_2)\rangle_c\langle\Phi(\hat{x}_3)\rangle \\
&+\langle T\Phi(\hat{x}_1)\Phi(\hat{x}_3)\rangle_c\langle\Phi(\hat{x}_2)\rangle + \langle T\Phi(\hat{x}_2)\Phi(\hat{x}_3)\rangle_c\langle\Phi(\hat{x}_1)\rangle + \langle\Phi(\hat{x}_1)\rangle\langle\Phi(\hat{x}_2)\rangle\langle\Phi(\hat{x}_3)\rangle\,,\;\ldots\;.
\end{aligned}$$

(28)

The expressions for equal-time Green functions are obtained by taking the well-defined equal-time limit which yields the appropriate operator ordering in the cluster expansions. We arrive at

$$\langle\Phi(x)\rangle \;=\; \langle\Phi(x)\rangle_c \;, \quad \langle\Pi(x)\rangle \;=\; \langle\Pi(x)\rangle_c \;,$$

$$\langle\Phi(x_1)\Phi(x_2)\rangle = \langle\Phi(x_1)\Phi(x_2)\rangle_c + \langle\Phi(x_1)\rangle\langle\Phi(x_2)\rangle \ ,$$

$$\langle\Pi(x_1)\Phi(x_2)\rangle = \langle\Pi(x_1)\Phi(x_2)\rangle_c + \langle\Pi(x_1)\rangle\langle\Phi(x_2)\rangle \ ,$$

$$\langle\Pi(x_1)\Pi(x_2)\rangle = \langle\Pi(x_1)\Pi(x_2)\rangle_c + \langle\Pi(x_1)\rangle\langle\Pi(x_2)\rangle \ ,$$

$$\begin{aligned}\langle\Phi(x_1)\Phi(x_2)\Phi(x_3)\rangle \ &= \ \langle\Phi(x_1)\Phi(x_2)\Phi(x_3)\rangle_c + \langle\Phi(x_1)\Phi(x_2)\rangle_c\langle\Phi(x_3)\rangle \\ &+\langle\Phi(x_1)\Phi(x_3)\rangle_c\langle\Phi(x_2)\rangle + \langle\Phi(x_2)\Phi(x_3)\rangle_c\langle\Phi(x_1)\rangle + \langle\Phi(x_1)\rangle\langle\Phi(x_2)\rangle\langle\Phi(x_3)\rangle \ , \ \ ... \ ,\end{aligned}$$

(29)

where all (equal) time arguments have been suppressed. In view of their length the cluster expansions for the other Green functions required for our calculations are not explicitly given here, but can be found in [1]. The explicit forms of the cluster expansions of $\langle \mathrm{x}^n\rangle$, $n = 1, \cdots, 6$ (required for our analysis in $(0+1)$ dimensions) are given in appendix B.

B Cluster expansion of $\langle \mathrm{x}^n\rangle$

Applying the derivation of appendix A, we obtain the following expressions for the cluster expansion of $\langle \mathrm{x}^n\rangle$, $n = 1, \cdots, 6$ in Φ^4_{0+1}-theory using $\Phi(x) \to \mathrm{x}$:

$$\langle \mathrm{x}\rangle = \langle \mathrm{x}\rangle_c \ , \tag{30}$$

$$\langle \mathrm{x}^2\rangle = \langle \mathrm{x}\rangle_c^2 + \langle \mathrm{x}^2\rangle_c \ , \tag{31}$$

$$\langle \mathrm{x}^3\rangle = \langle \mathrm{x}\rangle_c^3 + 3\langle \mathrm{x}\rangle_c\langle \mathrm{x}^2\rangle_c + \langle \mathrm{x}^3\rangle_c \ , \tag{32}$$

$$\langle \mathrm{x}^4\rangle = \langle \mathrm{x}\rangle_c^4 + 6\langle \mathrm{x}\rangle_c^2\langle \mathrm{x}^2\rangle_c + 3\langle \mathrm{x}^2\rangle_c^2 + 4\langle \mathrm{x}\rangle_c\langle \mathrm{x}^3\rangle_c + \langle \mathrm{x}^4\rangle_c \ , \tag{33}$$

$$\begin{aligned}\langle \mathrm{x}^5\rangle = \langle \mathrm{x}\rangle_c^5 + 10\langle \mathrm{x}\rangle_c^3\langle \mathrm{x}^2\rangle_c + 15\langle \mathrm{x}\rangle_c\langle \mathrm{x}^2\rangle_c^2 + 10\langle \mathrm{x}\rangle_c^2\langle \mathrm{x}^3\rangle_c + 10\langle \mathrm{x}^2\rangle_c\langle \mathrm{x}^3\rangle_c \\ +5\langle \mathrm{x}\rangle_c\langle \mathrm{x}^4\rangle_c + \langle \mathrm{x}^5\rangle_c \ ,\end{aligned} \tag{34}$$

$$\begin{aligned}\langle \mathrm{x}^6\rangle = \langle \mathrm{x}\rangle_c^6 + 15\langle \mathrm{x}\rangle_c^4\langle \mathrm{x}^2\rangle_c + 45\langle \mathrm{x}\rangle_c^2\langle \mathrm{x}^2\rangle_c^2 + 15\langle \mathrm{x}^2\rangle_c^3 + 20\langle \mathrm{x}\rangle_c^3\langle \mathrm{x}^3\rangle_c \\ +60\langle \mathrm{x}\rangle_c\langle \mathrm{x}^2\rangle_c\langle \mathrm{x}^3\rangle_c + 10\langle \mathrm{x}^3\rangle_c^2 + 15\langle \mathrm{x}\rangle_c^2\langle \mathrm{x}^4\rangle_c + 15\langle \mathrm{x}^2\rangle_c\langle \mathrm{x}^4\rangle_c + 6\langle \mathrm{x}\rangle_c\langle \mathrm{x}^5\rangle_c + \langle \mathrm{x}^6\rangle_c \ .\end{aligned} \tag{35}$$

C The GEP approximation in $(0+1)$ dimensions

We consider the Hamiltonian

$$H = \frac{1}{2}\mathrm{p}^2 + \frac{1}{2}m^2\mathrm{x}^2 + \frac{1}{4}\lambda\mathrm{x}^4 = \frac{1}{2}p^2 + \frac{1}{2}m^2(x+\mathrm{x}_0)^2 + \frac{1}{4}\lambda(x+\mathrm{x}_0)^4 \ , \tag{36}$$

where m^2 can be positive or negative. The GEP (Gaussian effective potential) in $(0+1)$ dimensions is given by a constrained variational calculation with a Gaussian trial wave function, i.e. by the ansatz

$$\Psi_{\mathrm{x}_0}(x) = \left(\frac{M}{\pi}\right)^{\frac{1}{4}} e^{-\frac{M}{2}x^2} \ . \tag{37}$$

This ansatz can then be seen as the ground state of a variational harmonic Hamiltonian of the form

$$H = \frac{1}{2}p^2 + \frac{1}{2}M^2x^2 \tag{38}$$

with an effective mass M. The connection to the field theoretical Hartree-Fock-Bogoliubov ansatz becomes obvious by noting, that (37) is the quasiparticle vacuum with respect to Bogoliubov-transformed creation and annihilation operators. Keeping this last point in mind, it is also straightforward to see why in a Gaussian trial state all connected Green functions of higher order than the two-point function vanish; this property follows directly from Wick's theorem.

The resulting equation for the effective mass is

$$M^2 - m^2 = 3\lambda\left(\mathrm{x}_0^2 + \frac{1}{2M}\right) \ , \tag{39}$$

which is equivalent to the Gap equation following from the Bogoliubov-ansatz.

References

[1] Wang, S.J., Cassing, W., Häuser, J.M., Peter, A., Thoma, M.H.: Ann. Phys. **242**, 235 (1995)

[2] Chang, S.J.: Phys. Rev. **D12**, 1071 (1975); Phys. Rev. **D13**, 2778 (1976)

[3] Funke, M., Kaulfuss, U., Kümmel, H.: Phys. Rev. **D35**, 621 (1987)

[4] Harindranath, A., Vary, J.P.: Phys. Rev. **D36**, 1141 (1987); Phys. Rev. **D37**, 1076 (1988)

[5] Polley, L., Ritschel, U.: Phys. Lett. **B221**, 44 (1989)

[6] Thoma, M.H.: Z. Phys. **C44**, 343 (1989)

[7] Stevenson, P.M.: Phys. Rev. **D32**, 1389 (1985)

[8] Stancu, I., Stevenson, P.M.: Phys. Rev. **D42**, 2710 (1990); Stancu, I: Phys. Rev. **D43**, 1283 (1991)

[9] Cea, P.: Phys. Lett. **B236**, 191 (1990); Cea, P., Tedesco, L.: Phys. Lett. **B335**, 423 (1994)

[10] Magruder, S.F.: Phys. Rev. **D14**, 1602 (1976); Chang, S.J., Magruder, S.F.: Phys. Rev. **D16**, 983 (1977)

[11] Freedman, B., Smolensky, P., Weingarten, D.: Phys. Lett. **B113**, 481 (1982)

[12] Stevenson, P.M.: Z. Phys. **C24**, 87 (1984)

[13] Consoli, M., Stevenson, P.M.: Z. Phys. **C63**, 427 (1994); DE-FG05-92ER-40717-5, hep-ph/9303256; DE-FG05-92ER-40717-13, hep-ph/9403299; DE-FG05-92ER-40717-14, hep-ph/9407334

[14] Huang, K., Manousakis, E., Polonyi, J.: Phys. Rev. **D35**, 3187 (1987)

[15] Häuser, J.M., Cassing, W., Peter, A., Thoma, M.H.: Z. Phys. **A353**, 301 (1995)

[16] Peter, A., Häuser, J.M., Thoma, M.H., Cassing, W.: Z. Phys. **C71**, 515 (1996)

[17] Wang, S.J., Cassing, W.: Ann. Phys. **159**, 328 (1985)

[18] Schmitt, K.J., Reinhard, P.G., Toepffer, C.: Z. Phys. **A336**, 123 (1990)

[19] Gherega, T., Krieg, R., Reinhard, P.G., Toepffer, C.: Nucl. Phys. **A560**, 166 (1993)

[20] Pfitzner, A., Cassing, W., Peter, A.: Nucl. Phys. **A577**, 753 (1994)

[21] Thoma, M.H.: Z. Phys. **C53**, 637 (1992)

[22] Amit, D.J.: *Field theory, the renormalization group and critical phenomena*, McGraw-Hill (1978)

[23] Derrick, G.H.: J. Math. Phys. **5**, 1252 (1964)

Figure Captions

fig.1: The ratios $|\langle \mathrm{x}^n \rangle_c / \langle \mathrm{x}^n \rangle|$ for n=2,...,6 as a function of $\mathrm{x}_0/\sqrt{\mu} = \langle \mathrm{x} \rangle / \sqrt{\mu}$ for the double-well potential with $\lambda/(4\mu^3) = 0.0158$ (upper two pictures) and for the anharmonic oscillator potential with $\lambda/(4m^3) = 10$ (lower two pictures). L.h.s.: exact results; r.h.s.: results within the $\Phi^4_{0+1}CD(2,3,4,5,6)$-approximation obtained by time dependently switching on the residual interaction.

fig.2: Absolute squares of the ground state wave function $\Psi_0(\mathrm{x})$ and the wavefunction of the first excited state $\Psi_1(\mathrm{x})$ (both obtained from the exact solution) as a function of x and of $f(J) = \langle \Psi_0 | \mathrm{x} | \Psi_0 \rangle$ in the case of a double-well potential with $\lambda/(4\mu^3) = 0.0158$ and an external source J.

fig.3: Qualitative picture of the external source J as a function of $\mathrm{x}_0 = \langle \mathrm{x} \rangle$ for 3 different cases: (1) no symmetry breaking, (2) Maxwell construction in case of symmetry breaking, (3) analytical continuation into the two phase region of the Maxwell contruction in case of symmetry breaking.

fig.4: External source J as a function of $\mathrm{x}_0/\sqrt{\mu}$ in $\Phi^4_{0+1}CD(2,3,4,5,6)$-approximation for a double-well potential with $\lambda/(4\mu^3) = 0.0158$; x_0 is changed in time according to $\mathrm{x}_0(t)/\sqrt{\mu} = \mathrm{x}_0^{start}/\sqrt{\mu} - \alpha t$. The fat solid line is the result in $\Phi^4_{0+1}CD(2)$-approximation with $\alpha = 0.00001$ c/fm ($\mu^2 = 1$ MeV^2).

fig.5: The ratios $\left| \sum_{\alpha\beta} \langle \Phi_\alpha \Phi_\beta \rangle_c \,/\, \sum_{\alpha\beta} \langle \Phi_\alpha \Phi_\beta \rangle \right|$ $(n = 2)$, $\left| \sum_{\alpha\beta\gamma} \langle \Phi_\alpha \Phi_\beta \Phi_\gamma \rangle_c \,/\, \sum_{\alpha\beta\gamma} \langle \Phi_\alpha \Phi_\beta \Phi_\gamma \rangle \right|$ $(n = 3)$ and $\left| \sum_{\alpha\beta\gamma\delta} \langle \Phi_\alpha \Phi_\beta \Phi_\gamma \Phi_\delta \rangle_c \,/\, \sum_{\alpha\beta\gamma\delta} \langle \Phi_\alpha \Phi_\beta \Phi_\gamma \Phi_\delta \rangle \right|$ $(n = 4)$ as a function of $\Phi_0 = \langle \Phi(x) \rangle$ for $(1+1)$ (l.h.s.) and $(2+1)$ (r.h.s.) dimensions in $\Phi^4 CD(2,3,4)$-approximation; all results have been obtained by switching on the coupling adiabatically.

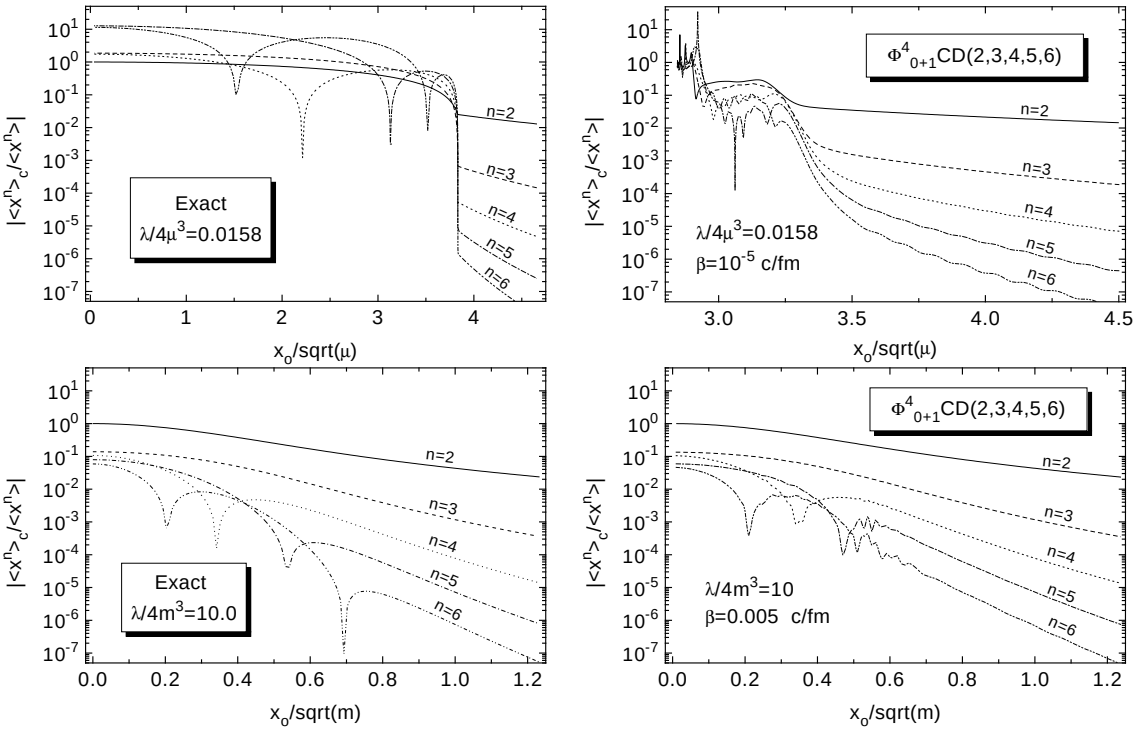
Exact
λ/4μ³=0.0158
Φ⁴₀₊₁CD(2,3,4,5,6)
λ/4μ³=0.0158
β=10⁻⁵ c/fm
Exact
λ/4m³=10.0
Φ⁴₀₊₁CD(2,3,4,5,6)
λ/4m³=10
β=0.005 c/fm
n=2
n=3
n=4
n=5
n=6
|<xⁿ>c/<xⁿ>|
x0/sqrt(μ)
x0/sqrt(m)

Figure 1:

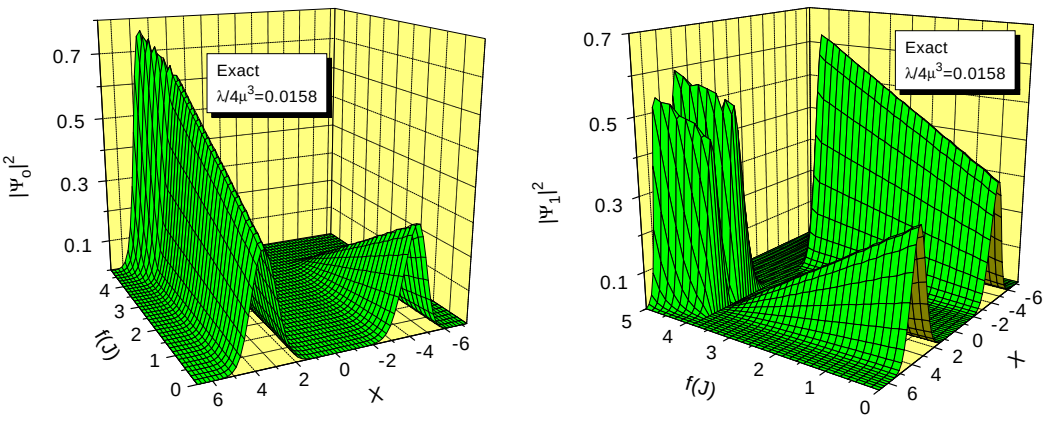

Figure 2:

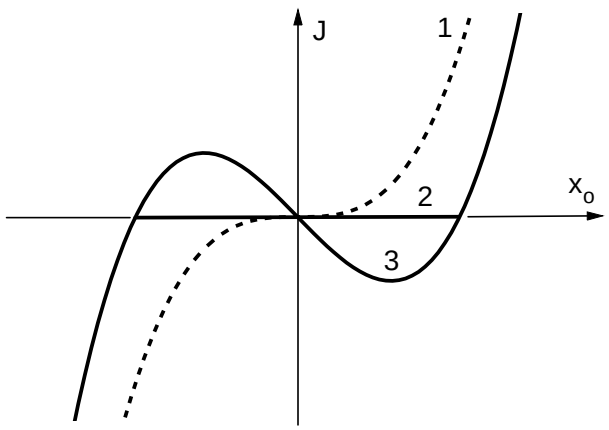

Figure 3:

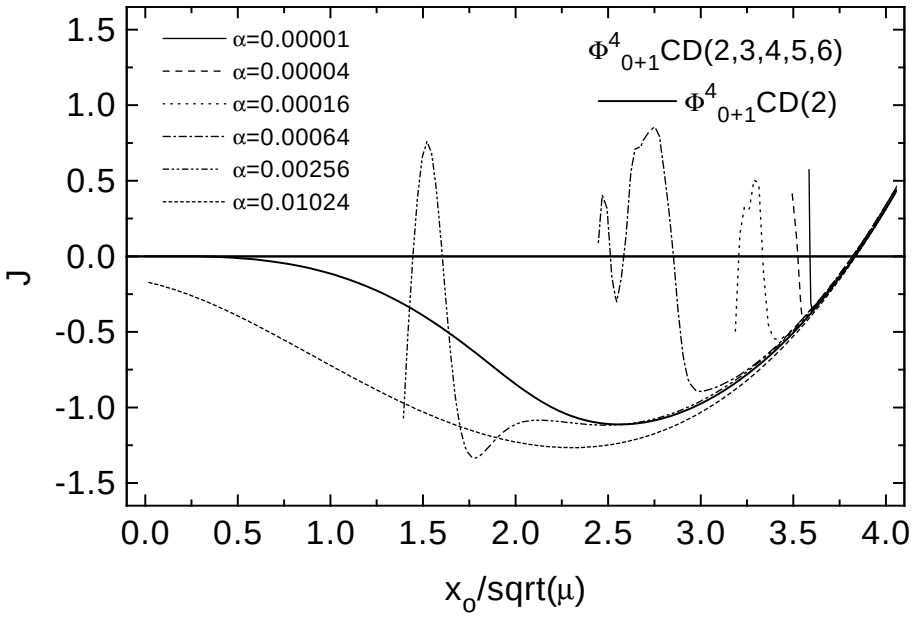
α=0.00001
α=0.00004
α=0.00016
α=0.00064
α=0.00256
α=0.01024
Φ4 0+1CD(2,3,4,5,6)
Φ4 0+1CD(2)
J
xo/sqrt(μ)
1.5
1.0
0.5
0.0
-0.5
-1.0
-1.5
0.0
0.5
1.0
1.5
2.0
2.5
3.0
3.5
4.0

Figure 4:

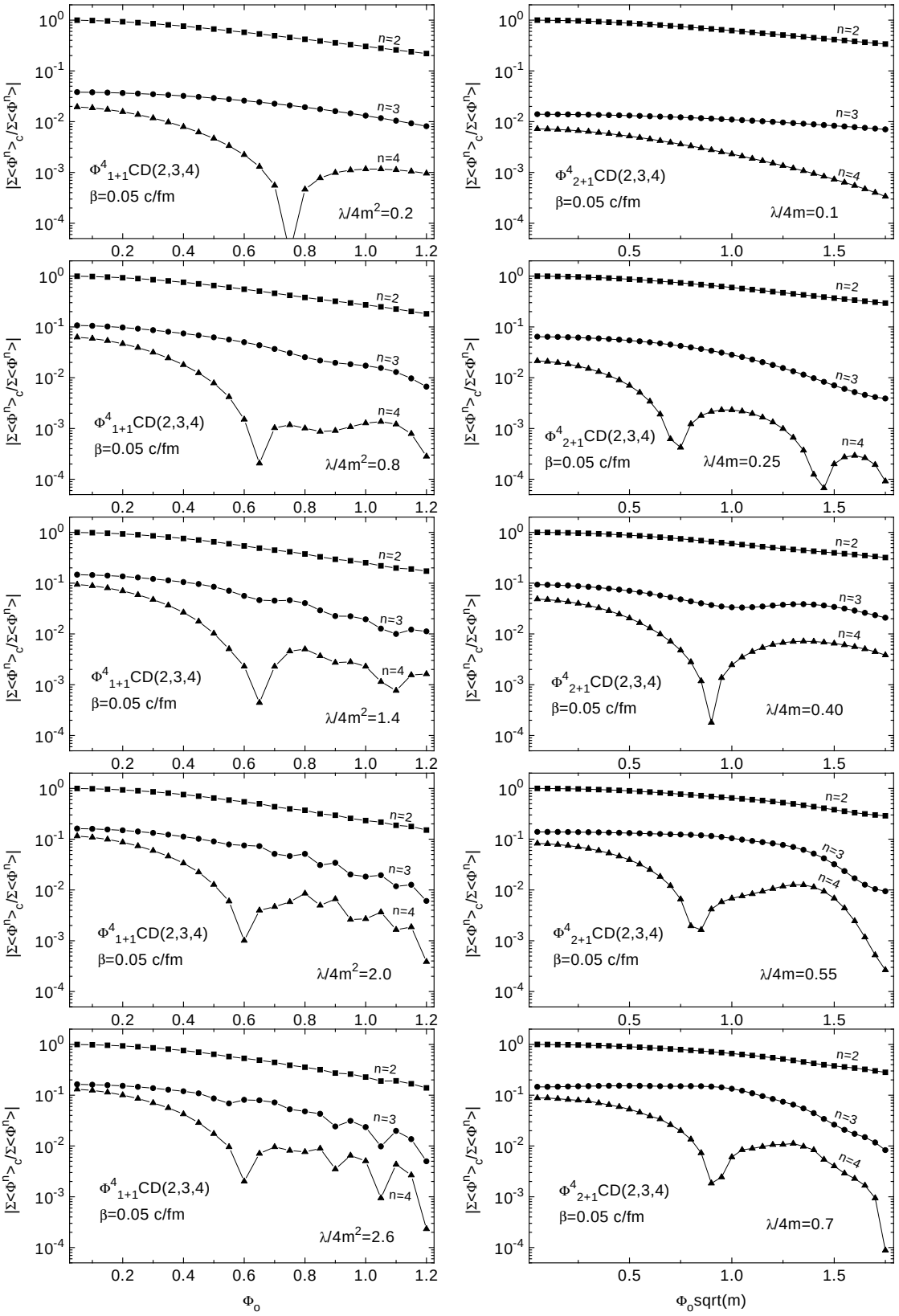
Φ^4_{1+1}CD(2,3,4)
β=0.05 c/fm
λ/4m²=0.2
λ/4m²=0.8
λ/4m²=1.4
λ/4m²=2.0
λ/4m²=2.6
Φ^4_{2+1}CD(2,3,4)
β=0.05 c/fm
λ/4m=0.1
λ/4m=0.25
λ/4m=0.40
λ/4m=0.55
λ/4m=0.7
n=2
n=3
n=4
$|\langle\Phi^n\rangle\langle\Sigma\rangle/\langle\Sigma^2\rangle\langle\Phi^n\rangle\langle\Sigma\rangle|$
Φ_o
$\Phi_o$sqrt(m)

Figure 5: